Assessment of the inhibition of Dengue virus infection by carrageenan via real-time monitoring of cellular oxygen consumption rates within a microfluidic device

Shih-Hao Huang,[1,2,a)] Yi-Syun Lin,[1] Chih-Wei Wu,[1] and Chang-Jer Wu[3]
[1]*Department of Mechanical and Mechatronic Engineering, National Taiwan Ocean University, Keelung 202-24, Taiwan*
[2]*Center for Marine Mechatronic Systems (CMMS), Center of Excellence for the Oceans (CEO), National Taiwan Ocean University, Keelung 202-24, Taiwan*
[3]*Department of Food Science, National Taiwan Ocean University, Keelung 202-24, Taiwan*

(Received 20 February 2014; accepted 27 March 2014; published online 8 April 2014)

A microfluidic device combined with a light modulation system was developed to assess the inhibitory effect of carrageenan on Dengue virus (DENV) infection via real-time monitoring of cellular oxygen consumption rates (OCRs). Measuring cellular OCRs, which can reflect cellular metabolic activity, enabled us to monitor the process of viral infection in real time and to rapidly determine the antiviral activity of potential drugs/chemical compounds. The time variation of the cellular OCR of single cells that were infected *in situ* by DENV at different multiplicity of infection (m.o.i.) values was first successfully measured within a microfluidic device. The influence of the timing of carrageenan treatment on DENV infection was then examined by real-time monitoring of cellular OCRs in three groups. Cells that were pre-treated with carrageenan and then infected with DENV served as a pre-treatment group, cells to which carrageenan was added simultaneously with DENV served as a virucide group, and cells that were pre-infected with DENV and then treated with carrageenan served as a post-treatment group. By monitoring cellular OCRs, we could rapidly evaluate the inhibitory effect of carrageenan on DENV infection, obtaining a result within 7 h and showing that carrageenan had strong and effective anti-DENV activity in the three groups. In particular, a strong inhibitory effect was observed in the virucide group. Moreover, once the virus enters host cells in the post-treatment group, the immediate treatment with carrageenan for the infected cells has higher efficiency of antiviral activity. Our proposed platform enables to perform time-course or dose-response measurements of changes in cellular metabolic activity caused by diseases, chemical compounds, and drugs via monitoring of the cellular OCR, with rapid and real-time detection. This approach provides the potential to study a wide range of biological applications in cell-based biosensing, toxicology, and drug discovery.
 [http://dx.doi.org/10.1063/1.4870772]

I. INTRODUCTION

Dengue virus (DENV), a member of the genus *Flavivirus* in the family *Flaviviridae*, is the agent of the most prevalent arboviral disease in humans in the past few decades.[1] There are four serotypes (DENV-1 to DENV-4), which can cause a mild illness, known as dengue fever, or severe dengue hemorrhagic fever/dengue shock syndrome in humans. Despite the increasing incidence and emergence of dengue infections around the world, there are no antiviral agents or vaccines available against DENV. Recently, carrageenans extracted from red seaweeds have

[a)]Author to whom correspondence should be addressed. Electronic mail: shihhao@mail.ntou.edu.tw. Tel.: 886-2-24622192 ext. 3209. Fax: 886-2-24620836

been found to possess a broad range of biological activities, including antiviral, antitumor, immunomodulatory, and anticoagulant activities.[2] Among these activities, carrageenans were reported to have effective antiviral activity against certain pathogenic viruses, such as DENV type II (DENV-2),[3,4] influenza A (H1N1) virus,[5] and human enterovirus 71 (EV 71).[6]

Plaque reduction and virus yield inhibition assays are currently two of the effective conventional assays used in the first step of assessing the antiviral activities of potential drugs/chemical compounds against certain pathogenic viruses.[7] The effectiveness of potential drugs in reducing the plaque-forming units (pfu) of viruses compared with controls is an indicator of antiviral activity. However, the conventional methods for the evaluation of antiviral activity, such as plaque reduction assays, are not efficient or real-time assays. For example, more than 48 h of incubation is needed to count the number of plaques derived from an infectious virus. Another rapid and sensitive *in vitro* procedure for evaluating antiviral agents is the MTT (3-(4,5-dimethylthiazol-2-yl)-2,5-diphenyl tetrazolium bromide) assay, which is based on the spectrophotometrical assessment for viability of virus-infected cells via *in situ* reduction of a tetrazolium dye, and this assay has been proven to have similar sensitivity to the plaque reduction assay.[7] However, the standard MTT assay, which typically requires that treated and control cells be incubated with the MTT reagent for 2 to 4 h before absorbance measurement, can damage cells and cannot be used for time-course measurements to assess cellular metabolic activity rapidly and in real time. Moreover, a large number of virus particles are needed to cause a productive infection, which is a great challenge for the precious and rare samples. Thus, it is necessary to establish a miniaturized platform with low consumption of virus and of potential drugs for research on viral infection and drug discovery.

Recently, microfluidic platforms have been widely used in cell-based viral infection and virus detection, such as chip-based polymerase chain reaction (PCR),[8,9] microfluidic platforms with a virus concentration generator,[10] and microfluidic bioreactors[11] to enhance infection efficiency and improve detection sensitivity. In these virus detection techniques, virus samples are often obtained from the infection system at a certain time point, which interrupts the viral infection process. The dynamic behavior of the viral infection process in live cells has not been studied in real time and *in situ* in these techniques. Development of real-time and *in situ* techniques is the current challenge forward in revealing viral infection mechanism to develop into antiviral agents. To this end, Zhang *et al.* proposed a three-layer microfluidic chip to monitor the infection process of a recombinant green fluorescent protein-Pseudorabies virus (GFP-PrV), which expressed GFP during genome replication, in real time *in situ*.[12] The viral infection process was monitored by tracking the fluorescence intensity of GFP. Although GFP-PrV has significant homology to the infectious viruses that serve as human pathogens, the recombinant process of GFP-PrV with GFP as a marker altered the genomic dsDNA of PrV, which might essentially influence the infectious nature of PrV.

In cellular assays and bioreactors, the rapid determination of cell viability is frequently accomplished by monitoring cellular metabolic activity via oxygen consumption. Monitoring cellular oxygen consumption provides useful information when studying critical biochemical pathways, including those underlying mitochondrial function, apoptosis, metabolic alterations caused by various stimuli or diseases, and toxicological responses to various compounds.[13] Monitoring cellular oxygen consumption rates (OCRs), which can reflect cellular metabolic activity, enables us to quantitatively monitor the viral infection process in real time and to rapidly determine the antiviral activities of potential drugs/chemical compounds. No recombinant process of the targeted virus with GFP is needed to serve as a marker followed by tracking of the fluorescence. In our previous work, we developed a digital light modulation system that utilizes a modified commercial digital micromirror device (DMD) projector.[14,15] The system is equipped with a UV light-emitting diode as a light modulation source and spatially directs excited light toward a microwell array device to measure the OCR of single cells via phase-based phosphorescence lifetime detection. In this study, we attempted to assess the inhibitory effect of carrageenan on DENV infection via real-time monitoring of cellular OCRs in our proposed microfluidic device. Phase-based phosphorescence lifetime detection was selected as the preferred detection scheme for cellular OCR measurements. The influence of the timing of

carrageenan treatment on DENV infection was then examined by real-time monitoring of cellular OCRs in three groups: Cells that were pre-treated with carrageenan and then infected with DENV served as a pre-treatment group, cells to which carrageenan was added simultaneously with DENV served as a virucide group, and cells that were pre-infected with DENV and then treated with carrageenan served as a post-treatment group. By monitoring cellular OCRs, we can rapidly evaluate the inhibitory effect of carrageenan on DENV infection in real time, obtaining a result within 7 h.

II. MATERIALS AND METHODS

A. Principle of operation

The microfluidic device consists of a combination of two components: An array of glass microwells deposited with Pt(II) octaethylporphine (PtOEP) as the oxygen-sensitive luminescent layer and a microfluidic module with pneumatically actuated lids set above the microwells to controllably seal the microwells of interest, as shown in Fig. 1. A glass substrate with 2×2 arrays of etched microwells was seeded with a suitable solution of cells, yielding a cell

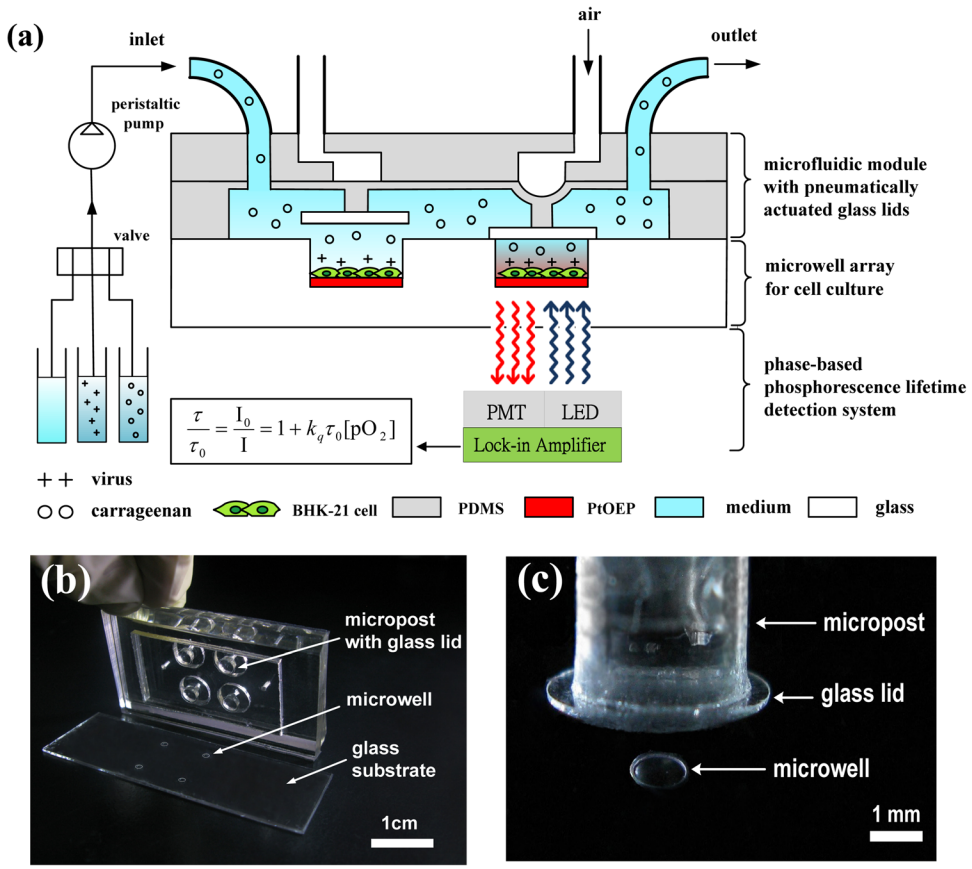

FIG. 1. A schematic of a microfluidic device combined with a light modulation system to assess the inhibitory effect of carrageenan on DENV infection via real-time monitoring of cellular OCRs by phase-based phosphorescence lifetime detection. The microfluidic device combines two components: An array of glass microwells deposited with PtOEP as the oxygen-sensitive luminescent layer and a microfluidic module with pneumatically actuated lids set above the microwells to controllably seal the microwells of interest. Long-term cellular OCR measurement was repeated over time using a periodic three-stage operation for replenishment of the microwells with fresh medium, entrapment of the chamber volume, and measurement of the oxygen concentration by lowering/raising the glass lids. (b) An image of the microfluidic device, which was assembled using three layers of PDMS structures that served as a microfluidic module and a glass substrate with 2×2 microwells inside a PDMS microchamber. (c) A close-up of one microwell with a pneumatically actuated lid set above it. The dimensions of the glass microwell were 1 mm in diameter and 50 μm in depth, which were etched into the soda-lime glass substrate.

monolayer adhered to the PtOEP layer within each microwell, as a proof of concept. After cell seeding, a microfluidic module with pneumatically actuated lids was set above the microwells to controllably seal the microwells of interest (Fig. 1(c)). More specifically, the air pressure system described in our previous work[15,16] was used to pneumatically actuate the glass lids (5 mm in diameter) to controllably seal the microwells. Briefly, a regulated compressed-air source was connected to multiple three-way solenoid valves (Lee, Inc., USA), where each valve was controlled by a custom LabVIEW program (National Instruments, Inc., USA) to switch rapidly between atmospheric pressure and input high pressure. High-pressure air was used to press a rounded glass lid attached to the end of a piston onto a single microwell to seal each microwell of interest (Fig. 2). The sealed microwell formed a small temporary chamber volume around the cells, which enables the rapid, real-time measurement of changes in the oxygen concentration. To measure the OCR of single cells with limited oxygen consumption, the cells must be isolated in a closed, small microwell to amplify the changes in oxygen consumption during an oxygen measurement. After release of the air pressure, the glass lids were raised to open the microwells and replenish the microwells with fresh medium. The microfluidic device was placed in an in-house incubation box mounted on an inverted microscope (IX-71, Olympus) to keep the temperature at 37 °C throughout the experiments. The microfluidic device was periodically perfused with fresh culture medium every 60 min through the inlet of the microfluidic module by a programmable peristaltic pump (TP-320, E-Chrom Tech Co., Taiwan) to maintain the survival of the single cells. For the assessment of the inhibition of DENV infection by carrageenan, an aqueous solution was introduced through the inlet of the microfluidic module at a specific point in time via a 3-to-1 four-way valve (PR4-NIPRO, Shineteh Instruments Co., Taiwan). The four-way valve enabled us to select a solution containing either carrageenan or

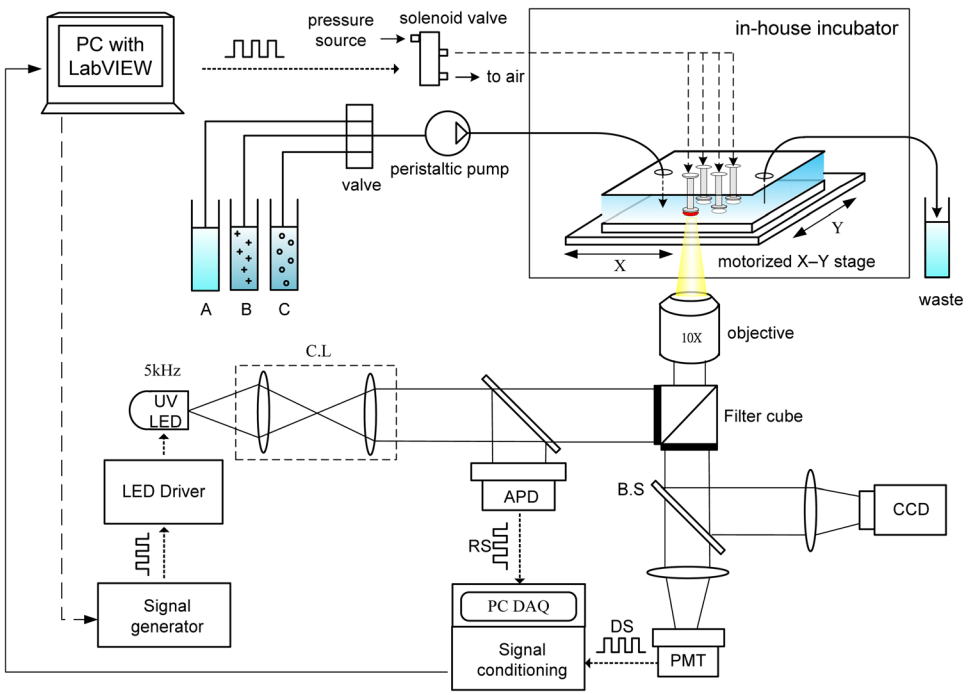

FIG. 2. A schematic of the light modulation system, equipped with a UV LED as the light modulation source to determine the cellular OCR via phase-based phosphorescence lifetime detection. A programmable motorized X-Y stage was used to spatially direct modulated 5 kHz excitation light toward a sealed microwell of interest. The phosphorescence lifetime (τ) was calculated by measuring the phase shift (θ) between the LED RS and the phosphorescence DS. The microfluidic device was placed in an in-house incubation box mounted on an inverted microscope. Multiple three-way solenoid valves, each was controlled by a custom LabVIEW program to switch rapidly between atmospheric and input pressures, were used to pneumatically actuate the glass lids to controllably seal the microwells. A peristaltic pump and four-way valve enabled the selection of aqueous solutions of (A) culture medium, (B) DENV, and (C) carrageenan to be directed toward the microfluidic device. (CL: collimating lens; BS: beam splitter; RS: reference signal; DS: detection signal; APD: amplified photodetector; and PMT: photo-multiplier tube).

DENV and to direct the solution toward to the microfluidic device to examine the influence of the timing of carrageenan treatment on DENV infection. Three groups were designed to assess the inhibitory effect of carrageenan on DENV infection via real-time monitoring of cellular OCRs. Cells that were pre-treated with carrageenan and then infected with DENV served as a pre-treatment group, cells to which carrageenan was added simultaneously with virus served as a virucide group, and cells that were pre-infected with DENV and then treated with carrageenan served as a post-treatment group.

B. Light modulation system for phase-based lifetime detection

A schematic of the light modulation system for phase-based phosphorescence lifetime detection is shown in Fig. 2. The light modulation system utilized a high-power UV light-emitting diode (LED) (390 nm, 3 W; EDISON OPTO) equipped with a collimating lens as the light modulation source, and a programmable motorized X-Y stage was used to spatially direct modulated 5 kHz excitation light toward a sealed microwell of interest to determine the cellular OCR via phase-based phosphorescence lifetime detection. The reference signal (RS) was recorded by measuring the light intensity of the modulated excitation light using an amplified photodetector (ET-2030A, Electro-Optics Technology, Inc.) via a 50/50 beam splitter (BS). The detection signal (DS) was recorded by simultaneously measuring the light intensity of the corresponding phosphorescence using a photomultiplier tube (PMT-R928, Hamamatsu) and a cooled CCD camera (CoolSNAP HQ^2, Photometrics) in real time, along with the LED RS. The LED RS and the phosphorescence DS were both recorded on a computer via a universal serial bus (USB) data acquisition (DAQ) card (USB-6251, National Instruments), followed by a signal conditioning process. The performance of our proposed oxygen-sensing devices, which was previously validated,[14] showed that the limit of detection of the dissolved oxygen (DO) in liquid was 0.02 ppm, dynamic range of DO was 0–30 ppm, accuracy of reading was less 6%, response time of PtOEP sensing layers was less than 1 s, and sensitivity was 8.2 in our Stern–Volmer calibration curve. Detailed descriptions of the facility setup, data acquisition, and phase-based phosphorescence lifetime detection have been reported in our previous work.[14,15,17]

C. Repeatable and long-term measurements of cellular OCRs

Measurement of the OCR of the cells cultivated on the PtOEP layer in the sealed microwells was performed by tracking the oxygen concentration in the cell medium over time via phase-based phosphorescence lifetime detection. The phosphorescence lifetime was calculated by measuring the phase shift (θ) between the LED RS (modulated excitation light) and the phosphorescence DS to calculate the luminescence lifetime (τ) via phase-based phosphorescence lifetime detection. The relationship between the phase shift (θ) and the lifetime (τ) can be approximated by the following formula:

$$\tan(\theta) = 2\pi\nu\tau, \tag{1}$$

where ν is the modulation frequency. In this study, a modulation frequency of $\nu = 5$ kHz was used to measure the luminescence decay time for phase-based phosphorescence lifetime detection. The phase shift (θ) between the RS and the DS was determined by digital lock-in analysis. The luminescent lifetime (τ) related to the dissolved oxygen concentration ($[O_2]$) is described by the Stern–Volmer relationship, as follows:

$$\frac{I_0}{I} = \frac{\tau_0}{\tau} = 1 + K_{SV}^S[O_2], \tag{2}$$

where I is the intensity, τ is the lifetime, K_{SV}^S is the Stern–Volmer constant for the solution, I_0 and τ_0 are the reference values in the absence of oxygen, and $[O_2]$ is the oxygen concentration in solution. To calculate transient changes in the OCR (OCR(t), $-d[O_2]/dt$), time-based differentiation was used to calculate $-d[O_2]/dt$ from the measured $[O_2]$ time-lapse data. The

measured [O_2] time-lapse data were filtered using a 7-point-wide, second-order polynomial, first-order derivative Savitzky–Golay kernel (0.107, 0.071, 0.036, 0, −0.036, −0.071, −0.107).[18]

To enable repeatable and long-term OCR measurements, each OCR measurement of the single cells inside a microwell was performed using a three-stage operation. In the first stage, denoted the O-stage, we raised the lid to unseal the microwell for several minutes by releasing the air pressure in the microfluidic module to replenish the microwell with fresh medium, thus re-equilibrating and restoring the cell to a normal status. In the second stage, denoted the S-stage, we lowered the lid to seal the microwell by applying air pressure and waiting for several minutes for the cell to stabilize before performing the OCR measurement. In the third stage, denoted the M-stage, we performed the OCR measurement for a preset period via phase-based phosphorescence lifetime detection. Long-term OCR measurement of the single cells was repeated over time by periodically repeating the three-stage operation of replenishing the microwell with fresh medium, sealing the microwell, and measuring the oxygen concentration. The duration of each stage was as follows: 60 s for the O-stage, 180 s for the S-stage, and 180 s for the M-stage, unless otherwise stated. The physiological state of the cells assessed, which was not adversely affected by the long-term cellular OCR measurements, has been previously confirmed.[15]

D. Fabrication of the microfluidic device

The microfluidic device combines two components: An array of glass microwells deposited with PtOEP and a microfluidic module with pneumatically actuated lids above the microwells to controllably seal the microwells of interest. The microfluidic device was assembled using three layers of polydimethylsiloxane (PDMS) structures to serve as a microfluidic module and a glass substrate with 2×2 microwells inside a PDMS microchamber (Fig. 1(b)). In this study, we fabricated 2×2 glass microwells that were 0.4, 0.6, 0.8, or 1 mm in diameter, 50 μm deep, and spaced 0.4, 0.6, or 1 mm apart. PtOEP ($\lambda_{ex} = 381$ nm, $\lambda_{em} = 646$ nm; Sigma-Aldrich, USA) was used as the oxygen-sensitive luminescent layer and was deposited into the microwells to monitor the oxygen concentration in each microwell. PtOEP displays strong phosphorescence at room temperature, with a high quantum yield and a long lifetime (ca. 100 μs). The glass substrate with 2×2 microwells was adhered to the microfluidic module using double-sided adhesive (410M, 3M, USA) for ease of operation. For long-term operation, the microfluidic module and glass substrate were clamped between two PMMA plates to prevent leakage. For detailed descriptions of the fabrication of the microfluidic module, please refer to our previous work on cellular OCR measurements.[14,15]

E. Cells, virus, and chemical compounds

Baby hamster kidney-21 (BHK-21) fibroblast cells were chosen as models of mammalian cells to perform the cellular OCR measurements in this study, due to these cells' higher oxygen consumption and susceptibility to infection by DENV. The other reason is that the DENV primarily infects the mammalian cells to induce intracellular virus multiplication, not in mosquito cells. Besides, three categories of carrageenans, kappa (κ), iota (ι), and lambda (λ) carrageenans, have been reported to block DENV-2 infection in mammalian cells, but only iota-carrageenans were virus inhibitors in mosquito cells (C6/36 HT cell lines).[4] The BHK-21 cells were cultured in 75 cm^2 tissue-culture Petri dishes at 37 °C in a humidified atmosphere of 5% CO_2/95% air. The BHK-21 cells were incubated in RPMI-1640 medium (1X liquid), which was supplemented with 5% bovine calf serum, 200 U/ml penicillin, and 200 μg/ml streptomycin. The cells were grown to preconfluence and passaged by trypsinization in a 0.5% trypsin/0.01% EDTA solution in phosphate buffered saline (PBS) for 5 min at 37 °C. After resuspension, the BHK-21 cells (1.0×10^6 cell/ml) were introduced into the microfluidic device, which was settled in an in-house incubator for cell culture at 37 °C with 5% CO_2 for 24 h. The diameter of the microwells ranged from 400 to 1000 μm, and each microwell contained approximately 480 to 1200 cells.

DENV-2 was chosen to infect the BHK-21 cells in this study. For simplification, "DENV" stands for "DENV-2" hereafter, unless otherwise stated. A local isolate (PL046) of DENV was

supplied by National Taiwan Ocean University (NTOU), Keelung, Taiwan. The PL046 strain of DENV was maintained in suckling mouse brains for the preparation of virus stocks and further experiments at the Laboratory Animal Facility at NTOU. Kappa carrageenan (the major component) was purchased from Sigma-Aldrich. "Carrageenan" stands for "kappa carrageenan" hereafter for simplification.

F. Inhibitory effect of carrageenan on viral infection

The influence of the timing of carrageenan treatment on DENV infection was examined by real-time monitoring of cellular OCRs in three groups, as follows:

(1) **Pre-treatment:** In total, 1 mg of carrageenan in 1 ml RPMI-1640 medium was first introduced into the microfluidic device through the inlet of the microfluidic module and incubated at 37 °C for 1 h in an in-house incubator mounted on an inverted microscope. Infectious DENV (multiplicity of infection (m.o.i.) = 1) was then introduced into the microfluidic device and incubated at 37 °C for 1 h. After incubation, both the carrageenan and unadsorbed virus were removed. We defined this stage as 0 h post-infection (0 hpi). The time variation of cellular OCR(t) in the pre-treatment group was then measured in real time within the microfluidic device.
(2) **Virucide group:** In total, 1 mg of carrageenan in 1 ml RPMI-1640 medium was mixed with an equal volume of DENV (m.o.i. = 1) in RPMI-1640 medium for 1 h. The mixture of carrageenan and DENV was then introduced into the microfluidic device and incubated at 37 °C for 1 h in an incubation box. After incubation, both the carrageenan and unadsorbed virus were removed; this stage was defined as 0 hpi. The remaining measurements were the same as those in the pre-treatment group.
(3) **Post-treatment group:** Infectious DENV (m.o.i. = 1) was first introduced into the microfluidic device and incubated at 37 °C for 1 h. Next, 1 mg of carrageenan in 1 ml RPMI-1640 medium was introduced into the microfluidic device and incubated at 37 °C for another 1 h. After incubation, both the carrageenan and unadsorbed virus were removed; this stage was defined as 0 hpi. The remaining measurements were the same as described above.

III. EXPERIMENTAL RESULTS AND DISCUSSION

A. OCR variation among the DENV-infected BHK-21 cells

To examine the feasibility of our proposed system for monitoring the viral infection process in real time via monitoring the OCR, BHK-21 cells were first infected *in situ* by DENV at different m.o.i. values in the microfluidic device. An m.o.i. is a ratio defined by the number of infectious virus particles deposited in a well divided by the number of target cells present in that well. After the BHK-21 cells were cultured on the PtOEP layer within the 2×2 glass microwells, which were 1 mm in diameter, an aqueous solution of DENV (m.o.i. = 0.1, 0.25, 0.5, or 1) was introduced into the microwells through the inlet of the microfluidic module and incubated at 37 °C for 1 h. After incubation, unabsorbed virus was removed, and the cells were replenished with culture medium for the OCR measurements.

Cell viability was determined using a live/dead assay (Invitrogen, CA) including calcein AM (live cells, green) and ethidium homodimer (dead cells, red). Typical fluorescence images of a microwell containing stained live/dead BHK-21 cells that were infected *in situ* by DENV at m.o.i. = 0.5 or 1 at 0, 5, and 10 hpi are shown in Fig. 3(a). At 0 hpi, the infected BHK-21 cells exhibited green fluorescence, and the cellular morphology was spindle shaped, indicating that the cells were still normal and alive at both m.o.i. = 0.5 and m.o.i. = 1. At 5 hpi, we observed a distinct cytopathic effect (CPE) on the infected cells, whose morphology became round. The CPE refers to damage to host cells during viral invasion because the infecting virus causes lysis (dissolution) of the host cells. The infected cells gradually became round and swollen at m.o.i. = 0.5 at 10 hpi, whereas most of the infected cells were dead (red fluorescence) at m.o.i. = 1 at 10 hpi. However, the fluorescent live/dead cell assay cannot exactly reflect

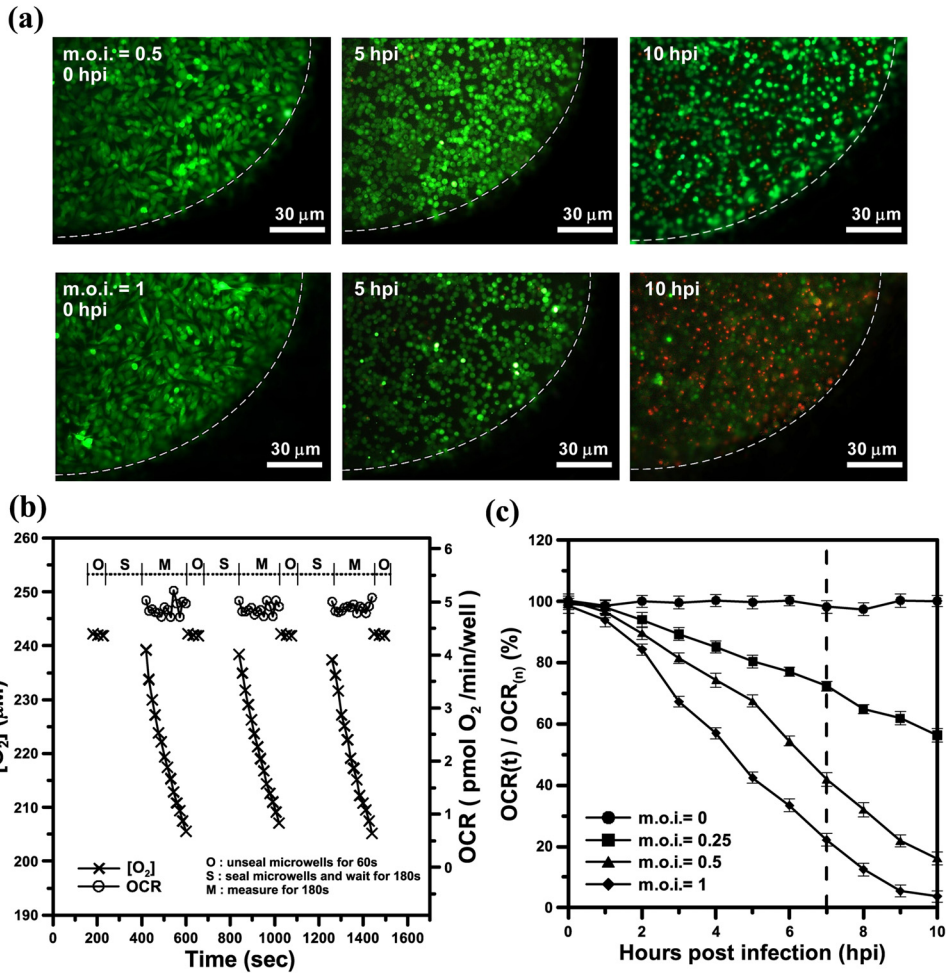

FIG. 3. (a) Typical fluorescence images of a microwell containing stained live/dead BHK-21 cells infected *in situ* by DENV at m.o.i. = 0.5 or 1 at 0, 5, and 10 hpi. The white dashed lines denoted the edge of the microwell. (b) The time variation of the aqueous oxygen concentration ($[O_2]$, μM) and OCR ($-d[O_2]/dt$) for normal BHK-21 cells within the microwells for three successive measurements by periodically sealing the glass microwell. (c) The time variation of the normalized OCR ($OCR(t)/OCR_{(n)}$, %) of the DENV-infected BHK-21 cells at different m.o.i. values within the microwells, as determined by periodic sealing of the microwells. The normalized OCR (OCR(t)/OCR(n), %) was measured at a 60 min time interval. Each OCR value included the three-stage operation for replenishment of the microwells with fresh medium (O-stage), entrapment of the chamber volume (S-stage), and measurement of the oxygen concentration (M-stage). $OCR_{(n)}$ denoted the averaged OCR value of normal BHK-21 cells (uninfected cells), which was 5 ± 0.1 pmol O_2/min/well for a long-term measurement (10 h).

metabolic dysfunction of mitochondrion for the damaged cells. Even if these DENV-infected cells are damaged for m.o.i. = 0.5 and 1 at 5 hpi, the live/dead cell assay still reflects the cells alive (green) as long as the plasma membranes of these cells did not becomes disrupted. The cell viability determined using the live/dead assay only qualitatively reflects the amount of viable cells, which does not reflect cellular metabolic activity in real time for infected living cells during the viral infection process. To this end, we quantitatively determined the time course of cellular metabolic activity via real-time monitoring of the OCR in our proposed platform.

Fig. 3(b) shows representative results of the aqueous oxygen concentration ($[O_2]$, μM) and OCR ($-d[O_2]/dt$) over time for normal BHK-21 cells within the microwells for three successive measurements by periodically sealing the glass microwell. At the start of the oxygen consumption measurement, we raised the lid for 60 s to replenish the microwell with fresh surrounding medium to re-equilibrate the cells to normal status (O-stage). During the O-stage, the aqueous oxygen concentration was maintained at an approximately constant value of 243 μM over time.

The lid was lowered to create a temporarily small, sealed chamber volume in the microwell during the S-stage. After waiting for 180 s for the cells to stabilize, we performed the phase-based phosphorescence lifetime detection for 180 s to measure the aqueous $[O_2]$ (M-stage). The aqueous $[O_2]$ gradually decreased with time during the M-stage. Using the microfluidic module to controllably seal the microwells, we successively performed three measurements by periodically sealing the glass microwell. Each measurement period involved the three-stage operation for replenishment of a microwell with fresh medium (O-stage), entrapment of the chamber volume (S-stage), and measurement of the oxygen concentration (M-stage). To calculate transient changes in the OCR(t), time-based differentiation was used to calculate $-d[O_2]/dt$ from the measured $[O_2]$ time-lapse data, as described in Sec. II C. The values of the OCR (t) were about 4.9 ± 0.1 pmol O_2/min/well, which did not vary significantly over time for three successive measurements. Repeatable and consistent measurements indicated that the oxygen measurements did not adversely affect the physiological state of the cells measured.

Fig. 3(c) shows the time variation of the normalized OCR ($OCR(t)/OCR_{(n)}$, %) of the DENV-infected BHK-21 cells at different m.o.i. values within the microwells, as determined by periodic sealing of the microwells. $OCR(t)/OCR_{(n)}$ was measured at a 60 min time interval. Each OCR value included the three-stage operation thorough O-stage, S-stage, and M-stage. $OCR_{(n)}$ denoted the averaged OCR value of normal BHK-21 cells (uninfected cells), which was 5 ± 0.3 pmol O_2/min/well for a long-term measurement (10 h). For the uninfected BHK-21 cells (m.o.i. = 0), $OCR(t)/OCR_{(n)}$ did not significantly vary over the 10 h period, indicating that the cells were in a normal physiological state during long-term and periodic OCR measurements within the sealed microwells. Although the fluorescent live/dead cell assay reflects the cells alive (green) for the damaged cells for m.o.i. = 0.5 and 1 at 5 hpi, $OCR(t)/OCR_{(n)}$ decreased from 100% to 70% and 45%, respectively. Our proposed platform can rapidly determine the cellular metabolic activity that is caused by DENV infection via monitoring of the OCR. For the DENV-infected BHK-21 cells at 10 hpi, $OCR(t)/OCR_{(n)}$ dramatically decreased from 100% to 56%, 16%, or 5% at m.o.i. = 0.25, 0.5, and 1, respectively. The infectious cells cause mitochondrial malfunction and decrease cellular metabolic activity, which is reflected by the OCR. When more cells were infected by DENV, $OCR(t)/OCR_{(n)}$ accordingly decreased over time.

B. Determination of the anti-DENV activity of carrageenan by OCR measurements

Before determining whether carrageenan has anti-DENV activity, we first assessed the cytotoxicity of carrageenan by OCR measurements, as this substance may possess unforeseen toxicity to cells. BHK-21 cells were treated and cultured with different concentrations of carrageenan (0 to 5 mg/ml) for 10 h. OCR measurements were then performed to assess cytotoxicity, as shown in Fig. 4(a). The result shows that the OCRs of the BHK-21 cells treated with the different concentrations of carrageenan were nearly constant in value after of 10 h treatment, which was nearly the same value as that of normal BHK-21 cells without carrageenan treatment. We can conclude that carrageenan posed no cytotoxicity to the cells tested. Next, we attempted to perform OCR measurements to determine whether carrageenan can interfere with virus-cell association.

Fig. 4(b) shows the normalized OCR ($OCR(t = 7\,hpi)/OCR_{(n)}$, %) of the DENV-infected BHK-21 cells at m.o.i. = 0–2 with or without pre-treatment with 1 mg/ml carrageenan. The anti-DENV activity of carrageenan was normalized and expressed as $OCR(t = 7\,hpi)/OCR_{(n)}$, where $OCR(t = 7\,hpi)$ and $OCR_{(n)}$ denoted the OCR value of the infected cells at 7 hpi and the averaged OCR value of normal cells without viral infection and carrageenan treatment, respectively. A higher value of $OCR(t = 7\,hpi)/OCR_{(n)}$ indicated higher efficiency of antiviral activity to inhibit DENV infection. As shown in Fig. 4(b), the $OCR(t = 7\,hpi)/OCR_{(n)}$ values of the infected BHK-21 cells with carrageenan treatment and infection at m.o.i. = 0 to 2 were all higher than those of the infected cells without carrageenan treatment. We can conclude that carrageenan has anti-DENV activity that inhibits infection with the virus. By monitoring the cellular OCR, we can rapidly evaluate the inhibitory effect of carrageenan on DENV infection,

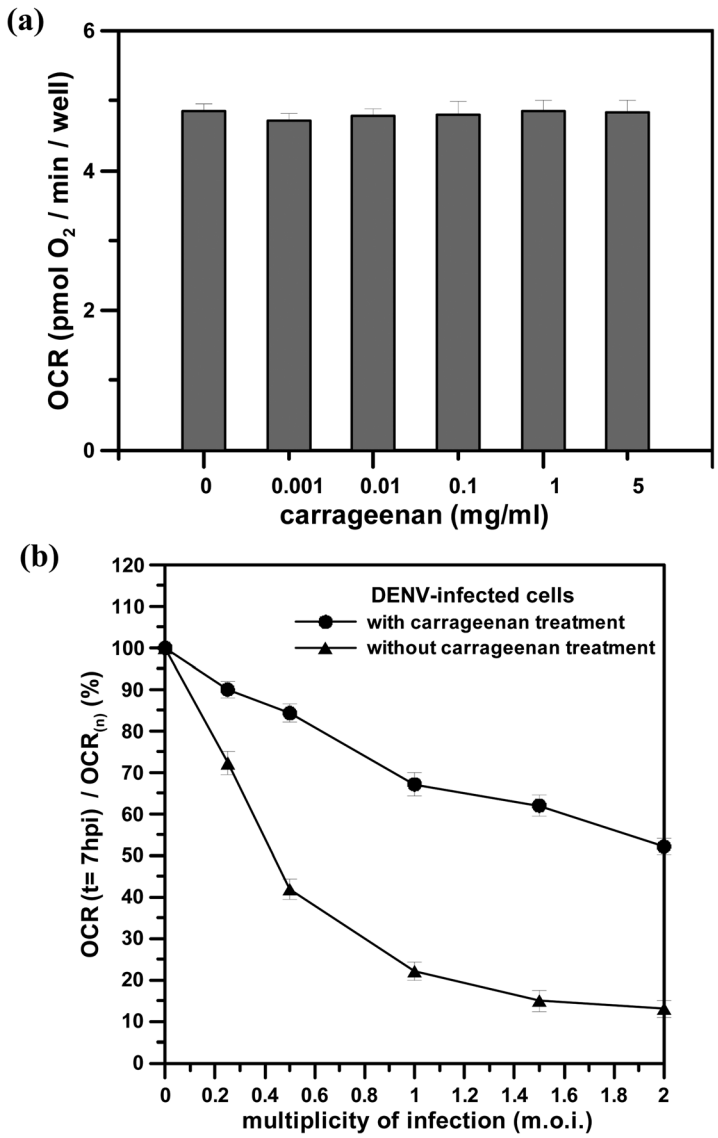

FIG. 4. (a) The OCR values of BHK-21 cells after 10 h of treatment with different concentrations of carrageenan. The error bar of each OCR value indicates three different measurements. (b) The normalized OCR (OCR(t = 7 hpi)/$OCR_{(n)}$, %) of DENV-infected BHK-21 cells at m.o.i. = 0 to 2 with or without pre-treatment with 1 mg/ml carrageenan. The anti-DENV activity of carrageenan was normalized and expressed as OCR(t = 7 hpi)/$OCR_{(n)}$, where OCR(t = 7 hpi) and $OCR_{(n)}$ denoted the OCR value of the infected cells at 7 hpi and the averaged OCR value of normal cells without viral infection and carrageenan treatment, respectively. The OCR(t = 7 hpi)/$OCR_{(n)}$ values of the infected BHK-21 cells without pre-treatment with carrageenan are denoted by a dashed line in Fig. 3(c).

obtaining a result in less than 7 h and showing that carrageenan has a strong and effective anti-DENV activity.

C. Influence of the timing of carrageenan treatment on DENV infectivity

The influence of the timing of carrageenan treatment on DENV infection was assessed by real-time monitoring of the cellular OCR in the pre-treatment group, virucide group, and post-treatment group, as shown in Fig. 5. BHK-21 cells that were pre-treated with carrageenan and then infected with DENV served as the pre-treatment group. BHK-21 cells that were treated with carrageenan simultaneously with DENV served as the virucide group. BHK-21 cells that were treated with carrageenan at 1 h after the adsorption of DENV to the cells served as the

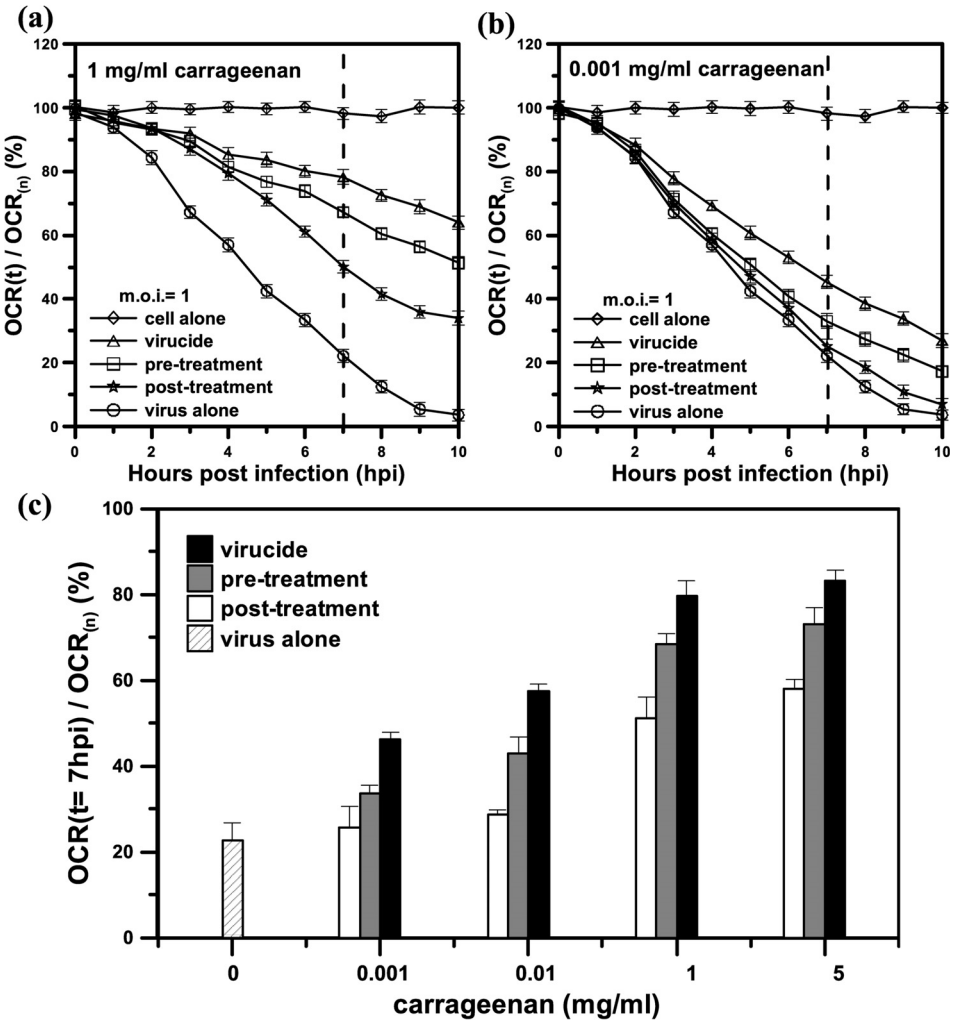

FIG. 5. The time variation of the normalized OCR ($OCR(t)/OCR_{(n)}$, %) of DENV-infected BHK-21 cells at m.o.i. = 1 and with (a) 1 mg/ml or (b) 0.001 mg/ml carrageenan treatment in the pre-treatment, virucide, and post-treatment groups. "virus alone" and "cell alone" denote the DENV-infected cells without treatment with carrageenan and uninfected cells, respectively. (c) The inhibition of DENV-infected BHK-21 cells at m.o.i. = 1 in the absence (virus alone) or presence of increasing concentrations of carrageenan, ranging from 0.001 to 1 mg/ml, in the pre-treatment, virucide, and post-treatment groups. The inhibitory effect was normalized and expressed as $OCR(t = 7\,hpi)/OCR_{(n)}$, %). The values of $OCR(t = 7\,hpi)/OCR_{(n)}$ for 1 and 0.001 mg/ml carrageenan treatment are denoted by a dashed line in (a) and (b). $OCR_{(n)}$ denoted the averaged OCR value of normal cells without viral infection and carrageenan treatment. Each value is the mean of triplicate assays ± standard deviation.

post-treatment group. Figs. 5(a) and 5(b) show the time variation of the normalized OCR ($OCR(t)/OCR_{(n)}$, %) of the DENV-infected BHK-21 cells at m.o.i. = 1 and with 1 or 0.001 mg/ml carrageenan treatment in the pre-treatment, virucide, and post-treatment groups. At 7 hpi (denoted by a dashed line), the normalized values ($OCR(t = 7\,hpi)/OCR_{(n)}$) in the pre-treatment, virucide, and post-treatment groups ranged between 20% and 100% for the virus alone (DENV-infected cells without treatment with carrageenan) and the cell alone (uninfected cells), respectively. This result indicated that carrageenan had strong and effective anti-DENV activity in the three groups. Notably, a strong inhibitory effect was observed in the virucide group (82%), which was better than the effects observed in the pre-treatment group (70%) and the post-treatment group (50%) (Fig. 5(a)). Moreover, the inhibitory effect in the three groups, which was normalized and expressed as $OCR(t = 7\,hpi)/OCR_{(n)}$, was proportional to the dose of added carrageenan, as shown in Fig. 5(c). A low carrageenan concentration (0.001 mg/ml) seemed to have no inhibitory effect (25%) in the post-treatment group, compared with the

effect (22%) of the virus alone, as shown in Figs. 5(b) and 5(c). Increasing the carrageenan concentration to 5 mg/ml did not show a significant five times better antiviral activity than that of 1 mg/ml. It seems that there is a saturation observed at a higher carrageenan concentration over 5 mg/ml. These results are consistent with previous work by our co-author's group, who used conventional plaque reduction to assess the inhibition of EV 71 infection by carrageenan.[6] However, the treated and control cells in their work needed 4 days of incubation and were then stained with 1% crystal violet to count the plaque number. Moreover, the inhibitory effects in these three groups were 92%, 87%, and 82%, respectively. The differences between the three groups were not significant due to the uncertainty of qualitative analysis based on counting plaque numbers. The conventional plaque reduction assay does not reflect the metabolic dysfunction of mitochondria in infected cells in real time. In contrast, our proposed system can rapidly determine the cellular metabolic activity that is caused by diseases and potential compounds via monitoring of the OCR rapidly and in real time. By monitoring the time variation of the cellular OCRs in real time for the pre-treatment group, virucide group, and post-treatment group, we can observe a significant inhibitory effect of carrageenan occurred in an early stage of DENV infection at 2 hpi as shown in Fig. 5(c). By monitoring the cellular OCRs, we can rapidly evaluate the inhibitory effect of carrageenan on DENV infection, obtaining a result within 7 h and showing that the virucide group experienced a strong inhibitory effect.

Sulfated polysaccharides, the major component of carrageenan, have been proven to affect the early stage of viral infection by virtue of interfering virus adsorption and internalization, which might be the mechanism of the antiviral activity of carrageenan against DENV infection.[3,6] In the pre-treatment group, the inhibition of DENV infection by carrageenan was attributed to the effect of the sulfated polysaccharides of carrageenan, which may block the virus-receptor binding sites on host cells to prevent viruses from entry into the host cells and the subsequent internalization of the nucleocapsid into the cytoplasm.[3,6] In the virucide group, the sulfated polysaccharides of carrageenan likely enabled direct binding to virus particles to form carrageenan-DENV complexes.[3,6] The formed carrageenan-DENV complexes are no longer able to interact with receptors on host cells to prevent viruses from entering the host cells via internalization into the cytoplasm. Although the virus-carrageenan complexes may still have been able to enter the cells, virions were likely not released from the endosomes to complete the infectious process. Carrageenan-DENV complexes can significantly deactivate or destroy the infectivity of viruses, which may be the reason that a stronger inhibitory effect was observed in the virucide group than in the pre-treatment and post-treatment groups. In the post-treatment group, upon addition of carrageenan after DENV entry into the host cells, carrageenan may have significantly affected viral RNA translation in the cytoplasm, suppressing the synthesis of viral proteins from the positive-strand RNA genome to reduce intracellular virus multiplication.[3,6]

Although the inhibitory effect in the post-treatment group was not better than the effects in the pre-treatment and virucide groups, the immediate treatment with carrageenan for the infected cells effectively increased the anti-DENV activity. Fig. 6 shows the influence of the time of addition of carrageenan in the post-treatment group. Carrageenan was added to the BHK-21 cells simultaneously with DENV or at hourly intervals after the adsorption of the virus to the host cells. The inhibitory effect was normalized and expressed as $(OCR_{treat} - OCR_{untreat})/OCR_{(n)}$ for the DENV-infected cells with and without carrageenan treatment compared with normal cells. OCR_{treat} and $OCR_{untreat}$ denoted the OCR values for the DENV-infected cells at m.o.i. = 1 and with and without treatment, respectively, with 1 mg/ml carrageenan. $OCR_{(n)}$ denoted the averaged OCR value of normal cells without viral infection and carrageenan treatment. A higher value of $(OCR_{treat} - OCR_{untreat})/OCR_{(n)}$ indicated higher efficiency of antiviral activity to inhibit DENV infection. As shown in Fig. 6, a strong inhibitory effect was observed when carrageenan was added to the cells together with the virus (time = 0 hpi) or immediately after virus adsorption (1 hpi). In contrast, no significant antiviral activity was observed when carrageenan was added after 3 hpi. These results reveal that carrageenan interferes with virus multiplication in a very early stage of the viral cycle, during the first hour of infection, and before the second hour of infection. Therefore, once the virus enters

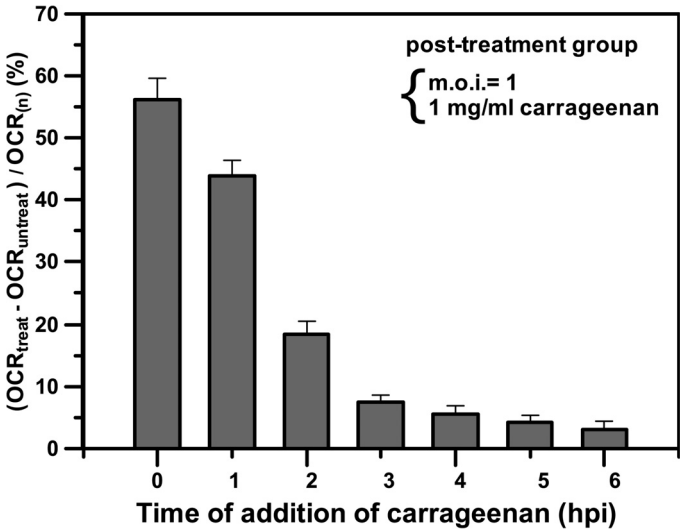

FIG. 6. The influence of the time of addition of carrageenan in the post-treatment group. Carrageenan was added to BHK-21 cells simultaneously with DENV or at hourly intervals after adsorption of the virus to the host cells. The inhibitory effect was normalized and expressed as $(OCR_{treat} - OCR_{untreat})/OCR_{(n)}$ for the DENV-infected cells with and without carrageenan treatment compared with normal cells. OCR_{treat} denoted the OCR value at 7 h after the addition of 1 mg/ml carrageenan to the DENV-infected cells at m.o.i. = 1. The control $OCR_{untreat}$ denoted the OCR value of the DENV-infected cells without carrageenan treatment at the same point in time. $OCR_{(n)}$ denoted the averaged OCR value of normal cells without viral infection and carrageenan treatment. Each value is the mean of triplicate assays ± standard deviation.

host cells in the post-treatment group, the immediate treatment with carrageenan for the infected cells has higher efficiency of antiviral activity to inhibit DENV infection.

In practical applications, carrageenan successfully ameliorated early symptoms of common cold and viral load in a recent clinical trial, favoring carrageenan a promising and suitable antiviral compound for safe and effective prevention of DENV infections.[19] However, larger clinical trials are still needed to study the therapeutic index in more detail. On the basis of our results above, the antiviral activity of carrageenan should effect in the early stage of virus infection by interfering with virus adsorption and internalization. We believe that once the DENV infection is confirmed, the immediate and persistent treatment with carrageenan would be the better therapeutic strategy, which could effectively improve the symptoms of DENV infections to prevent the patients from becoming worse. At the current stage, carrageenan may be suitable serving as a health food supplement for daily antiviral prevention.

IV. CONCLUSIONS

Our proposed platform provides the capability to perform time-course or dose-response measurements of changes in cellular metabolic activity that may be caused by diseases, chemical compounds, and drugs via rapid and real-time monitoring of the OCR. By monitoring the cellular OCR, we could rapidly evaluate the inhibitory effect of carrageenan on DENV infection, obtaining a result within 7 h and showing that carrageenan has strong and effective anti-DENV activity in the three groups. In particular, a strong inhibitory effect was observed in the virucide group. Our results also show that once the virus enters host cells in the post-treatment group, the immediate treatment with carrageenan for the infected cells has higher efficiency of antiviral activity. The proposed microfluidic device can be easily extended from the current proof-of-concept 2×2 glass microwells to large-scale microwell arrays (such as 24 or 96 microwells) for high-throughput drug discovery due to the device's ease of fabrication. We are now ongoing to perform a setup of microfluidic device with 24 microwells to analyze a large number of samples in parallel in a very short time by using an array of 24 optical fibers coupled with pulsed LEDs and the corresponding 24 optical fibers with photodiodes, as well as, the other components. The microfluidic device, which merely requires a low amount of virus to

cause a productive infection and a low amount of the tested drugs, provides the potential to study a wide range of biological applications in cell-based biosensing, toxicology, and drug discovery.

ACKNOWLEDGMENTS

This work was partially supported by the National Science Council, Taiwan, through Grant No. NSC 102-2221-E-019-015-MY2.

[1]D. J. Gubler, Trends Microbiol. **10**(2), 100–103 (2002).
[2]S. Patel, 3 Biotech **2**(3), 171–185 (2012).
[3]L. B. Talarico and E. B. Damonte, Virology **363**(2), 473–485 (2007).
[4]L. B. Talarico, M. D. Noseda, D. R. B. Ducatti, M. E. R. Duarte, and E. B. Damonte, J. Gen. Virol. **92**(6), 1332–1342 (2011).
[5]W. Wang, P. Zhang, C. Hao, X.-E. Zhang, Z.-Q. Cui, and H.-S. Guan, Antiviral Res. **92**(2), 237–246 (2011).
[6]Y.-H. Chiu, Y.-L. Chan, L.-W. Tsai, T.-L. Li, and C.-J. Wu, Antiviral Res. **95**(2), 128–134 (2012).
[7]D. Chattopadhyay, M. C. Sarkar, T. Chatterjee, R. S. Dey, P. Bag, S. Chakraborti, and M. T. H. Khan, New Biotechnol. **25**(5), 347–368 (2009).
[8]Y. Zhang and P. Ozdemir, Anal. Chim. Acta **638**(2), 115–125 (2009).
[9]P. J. Asiello and A. J. Baeumner, Lab Chip **11**(8), 1420–1430 (2011).
[10]G. M. Walker, M. S. Ozers, and D. J. Beebe, Sen. Actuators, B **98**(2–3), 347–355 (2004).
[11]H. N. Vu, Y. Li, M. Casali, D. Irimia, Z. Megeed, and M. L. Yarmush, Lab Chip **8**(1), 75–80 (2008).
[12]N. Xu, Z. F. Zhang, L. Wang, B. Gao, D. W. Pang, H. Z. Wang, and Z. L. Zhang, Biomicrofluidics **6**(3), 034122 (2012).
[13]J. Hynes, T. C. O'Riordan, J. Curtin, T. G. Cotter, and D. B. Papkovsky, J. Immunol. Methods **306**(1–2), 193–201 (2005).
[14]S.-H. Huang, C.-H. Tsai, C.-W. Wu, and C.-J. Wu, Sens. Actuators, A **165**(2), 139–146 (2011).
[15]S.-H. Huang, Y.-H. Hsu, C.-W. Wu, and C.-J. Wu, Biomicrofluidics **6**(4), 044118 (2012).
[16]S.-H. Huang, Z.-Y. Yu, K.-Y. Hung, and C.-K. Lin, J. Micro/Nanolithogr., MEMS, MOEMS **9**(4), 043002 (2010).
[17]S.-H. Huang, K.-S. Huang, C.-H. Yu, and H.-Y. Gong, Biomicrofluidics **7**(6), 064107 (2013).
[18]A. A. Gerencser, A. Neilson, S. W. Choi, U. Edman, N. Yadava, R. J. Oh, D. A. Ferrick, D. G. Nicholls, and M. D. Brand, Anal. Chem. **81**(16), 6868–6878 (2009).
[19]R. Eccles, C. Meier, M. Jawad, R. Weinmullner, A. Grassauer, and E. Prieschl-Grassauer, Respir. Res. **11**(1), 108 (2010).